

# Bioinspired Structural Material Exhibiting Post-Yield Lateral Expansion and Volumetric Energy Dissipation During Tension

By Lifeng Wang\* and Mary C. Boyce\*

Nature has inspired the design of improved synthetic materials that achieve superior and more efficient mechanical performance. Here microstructures inspired by the inner nacreous layer of seashells are designed and their mechanical properties including stiffness, strength, and energy dissipation are computed using micromechanical analysis. The hierarchical mineral/polymer microstructure can be tailored to achieve not only stiffness and strength, but also lateral plastic expansion during tension providing a volumetric energy dissipation mechanism.

## 1. Introduction

Biological materials, such as tooth, bone, and nacre, have developed complex, hierarchical, heterogeneous nanocomposites to provide superior mechanical properties. These composites are composed of large volume fractions of micron and sub-micron sized hard inorganic minerals embedded in or bonded together by a soft organic matrix.<sup>[1]</sup> The combination of hard and soft materials enables unusual combinations of outstanding mechanical performance properties including stiffness, strength, impact resistance, and toughness.<sup>[2]</sup> For example, nacre (the inner nacreous layer of mollusk shells) with ~95% mineral platelet content shows a work of fracture three orders of magnitude higher than that of the pure mineral itself.<sup>[3]</sup> Biological materials are also found to become insensitive to flaws due to the micro- and nanoscale size of mineral crystals,<sup>[3–5]</sup> where the small lengthscale of the mineral component averts their premature fracture. Dissipation and toughness are achieved primarily by the matrix deformation and, perhaps, by the mechanical sliding interaction of mineral bumps and bridges. After nacre deformation, the organic matrix layers of nacre have been observed to take the form of highly stretched polymer fibrils or ligaments bridging the plates<sup>[3,6]</sup> suggesting either an initial discreteness to the organic matrix or its breakup into the ligament structure during deformation enabling large axial stretching of ligaments as a dissipation mechanism.<sup>[7–9]</sup> A recent paper<sup>[10]</sup> has experimentally revealed the interesting

behavior of a post-yield lateral expansion of nacre during tension (essentially a negative “plastic” Poisson’s ratio), which shows plastic deformation is not incompressible; hence, there is a significant volumetric contribution to energy dissipation where part of the work of deformation is required to plastically expand the volume. They attribute the expansion to the interaction of mineral bumps or bridges between platelets, a dissipation mechanism suggested in earlier work.<sup>[11]</sup>

These remarkable structures and properties have inspired engineers and scientists to develop hierarchical nanocomposite materials that take advantage of the mechanical design principles found in nature.<sup>[12]</sup> Substantial progress has been made to develop bio-inspired materials such as clay/polymer nanocomposites<sup>[13,14]</sup> and ceramic/polymer hybrid materials.<sup>[15]</sup> Micromechanical studies have begun to explore the connections between the underlying structural features and the deformation mechanisms governing the superior properties.<sup>[8,16–18]</sup> However, it is still a challenge to identify the key and often subtle structural features that govern the mechanisms underlying the superior properties and to then fabricate synthetic composites that fully duplicate nature’s design, especially to achieve the combined strengthening and toughening mechanisms.

Recently, three-dimensional (3D) periodic polymer microframes<sup>[19,20]</sup> with sub-micrometer beams forming the frames have been found to exhibit unusual large plastic deformations when subjected to complex multiaxial loading conditions, with local failure strains reaching up to ~300%. Further study<sup>[21]</sup> reveals the role of the microstructural features in enabling a plasticity spreading mechanism during macroscopic loading, the development of a negative normal stress during simple shear, and a method of structuring a material to achieve desired mechanical performance. These unique characteristics make it possible to use these polymer structures as highly dissipative elements in lightweight energy absorption materials. The similarity in the deformed frame microstructures to the stretched matrix ligaments in the deformed nacre<sup>[3,6]</sup> suggests a possible role of this form of structured matrix in providing the superior mechanical performance.

In this paper, we investigate the mechanical performance of a structural composite material inspired by the inner nacreous layer of seashells using finite element based micro-mechanical analysis (FEA). The material consists of a layered “brick and mortar” form of microstructure with mineral bricks and a

[\*] Dr. L. F. Wang, Prof. M. C. Boyce  
Department of Mechanical Engineering  
Massachusetts Institute of Technology  
Cambridge, Massachusetts 02139 (USA)  
E-mail: wanglf@mit.edu; mcboyce@mit.edu

DOI: 10.1002/adfm.201000282

mortar of polymer microframes. We demonstrate that the discrete microframe polymer mortar provides the transfer of load to the bricks via the shear lag mechanism in a manner similar to a continuous matrix, giving the excellent stiffness and strength properties and their dependence on the aspect ratio of the bricks, the volume fraction of the mineral, and the effective shear behavior of the microframe. Furthermore, we reveal the polymer microframe mortar provides a lateral expansion during plastic deformation of the composite during tension (i.e., providing a mechanism that gives a negative “plastic” Poisson’s ratio as experimentally observed by Song et al.<sup>[10]</sup>). This macroscopic plastic lateral expansion and corresponding volumetric strain of the composite during tension result due to the evolution in the microframe mortar structure due to its local shearing deformation that gives stretching and rotation of microframe members.

## 2. Results and Discussion

The proposed hierarchical composite material consists of multilayered staggered mineral platelets embedded in polymer microframes with sub-micrometer feature size, as illustrated in **Figure 1**. The structures can be synthetically realized at the micron lengthscales or the millimeter lengthscale where the feature lengthscale would be tailored to meet the scale of the actual loading events. The two-dimensional micromechanical model consists of a representative volume element

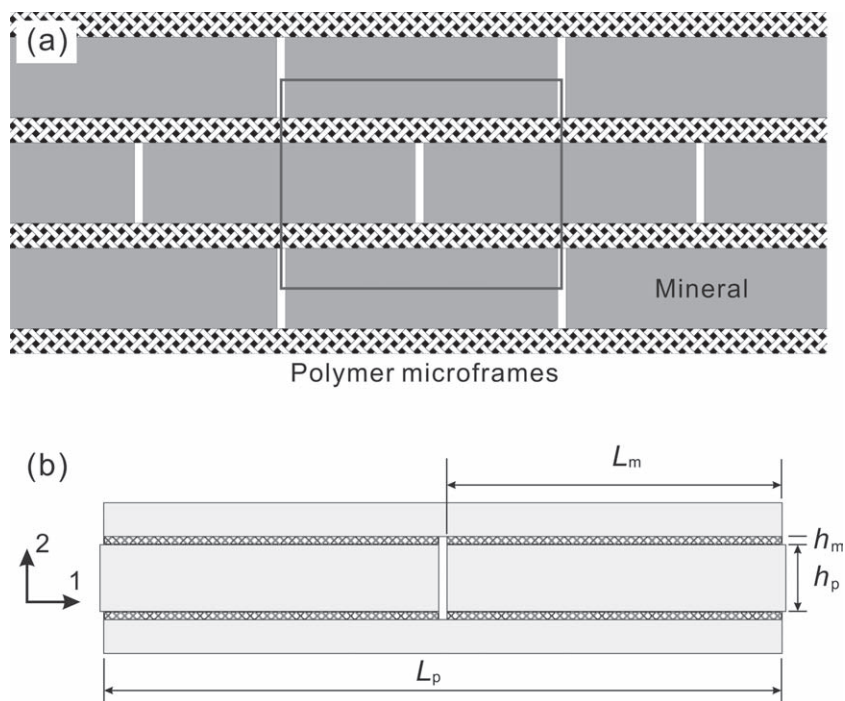


**Figure 1.** a) Schematic illustration of structural composite consisting of staggered mineral platelets and polymer microframes. b) 2D representative volume element (RVE) with platelet volume fraction of 0.90 and aspect ratio of 10. The key geometrical features include the microframe mortar thickness,  $h_m$ , the microframe member length,  $L_m$ , the brick thickness,  $h_p$ , and the brick length  $L_p$ .

(RVE) of the microstructure (Figure 1b). Periodic boundary conditions are applied to the RVE to capture the infinite periodic nature of the composite structure. Various RVEs of the composite structure are constructed in terms of the geometry features of mineral platelets, including the volume fraction ( $V_p$ ) and aspect ratio ( $s = L_p/h_p$ ). Figure 1b depicts an RVE with  $V_p = 90\%$  and  $s = 10$ , in which an idealized crisscross polymer microframe is taken. In the next simulations, we vary  $V_p$  at a fixed  $s$  and then vary  $s$  at a fixed  $V_p$  to study the effects of platelet volume fraction and platelet aspect ratio, respectively. The mineral brick is assigned a Young’s modulus of 100 GPa, an elastic Poisson’s ratio of 0.33, and a yield stress of 2 GPa.<sup>[14]</sup> The stress-strain behavior of the polymer is modeled using an elastic-viscoplastic constitutive model,<sup>[21]</sup> which captures the observed large strain features of glassy polymers; here we use the polymer behavior<sup>[21]</sup> that has a Young’s modulus of 3.3 GPa, an elastic Poisson’s ratio of 0.33, and a yield stress of 100 MPa.

The mechanical response of the composite structure under uniaxial tension for  $s = 10$  and  $0.50 < V_p < 0.90$  is depicted in **Figure 2**; for comparison purposes, nacre is observed to have an  $s \sim 10$  and  $V_p \sim 0.90$ – $0.95$ .<sup>[17,22]</sup> **Figure 3** depicts the corresponding contours of axial stress,  $\sigma_{11}$ , and shear stress,  $\sigma_{12}$ , for the cases with  $V_p = 0.90$ . The stiffness and yield strength increase with an increase in  $V_p$ . The stiffness and yield are achieved via the shear lag load transfer mechanism whereby shear of the mortar transfers axial stress to the mineral platelets as shown in Figure 3. The axial stress  $\sigma_{11}$  in the mineral platelets increases approxi-

mately linearly along the platelet length to a maximum stress of 200 MPa at the platelet midpoint. This stress build-up is a result of interfacial shear stress transmitted from the polymer microframe matrix as shown in the contours of shear stress  $\sigma_{12}$ , i.e., the shear lag load transfer mechanism. At a larger overall tensile strain of 1.0%, which is in the post-yield region, the axial stress in the platelet decreases but keeps the same approximately linear distribution because of the yielding of the polymer microframe. This phenomenon indicates the microframe provides the shear lag load transfer mechanism in a manner similar to a continuous matrix. Note that a double yield is observed in each tensile stress-strain curve because of multiple-yield events occurring in the microframe during loading. Immediately after yield, there follows a period of strain softening with the amount of softening increasing with increasing  $V_p$  (explained later).

The high mineral content together with the microstructure (high aspect ratio of mineral platelets bonded by organic matrix) provide the high mechanical performance (high stiffness, high strength, and high toughness) of natural nacre. However, such a high platelet concentration (~95%) is hard to achieve in synthetic composites (~20–30% of platelet volume fraction for a

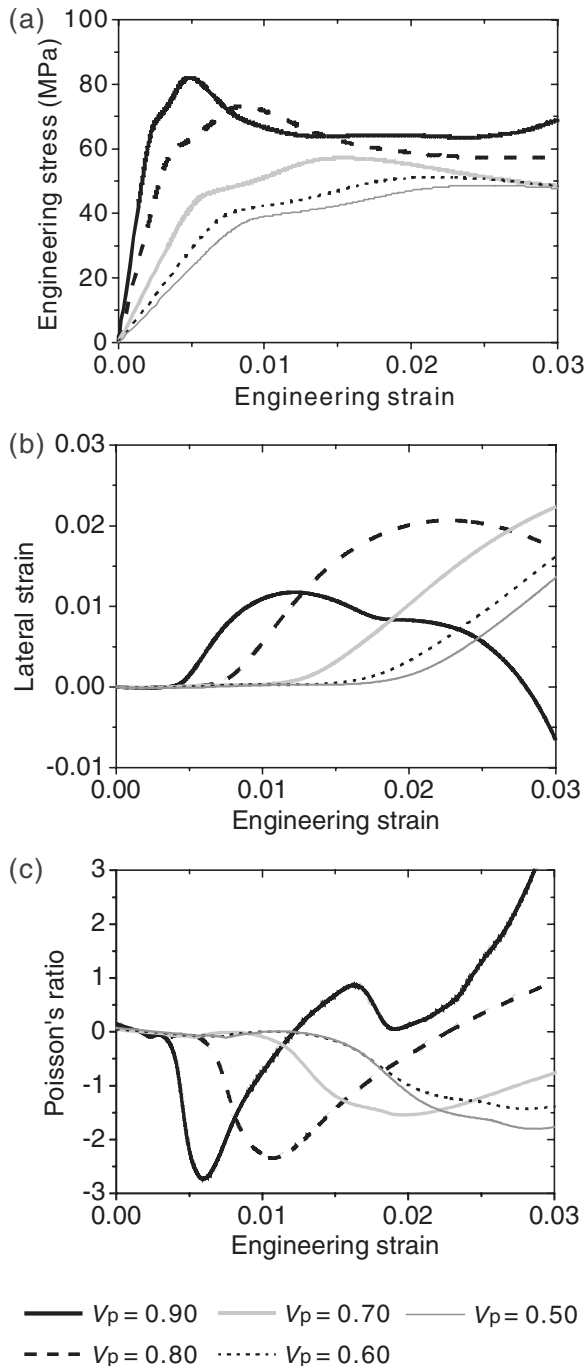


**Figure 2.** Mechanical response of the composite structure under uniaxial tension. a) Macroscopic tensile stress-strain curves for the composite for  $s = 10$  with various platelet volume fractions. b) The corresponding transverse strain versus tensile strain. c) The corresponding Poisson's ratio versus tensile strain.

nanocomposite,<sup>[13,14]</sup> up to 80% for a micrometer-scale composite<sup>[15]</sup>). Considering that a preferential (optimized) failure mode of the composite is one of platelet pull-out, the tensile strength of the composite material can be estimated by the shear lag model<sup>[23]</sup> as

$$\sigma_c = \frac{s}{2} V_p \tau_y \quad (1)$$

where  $\tau_y$  is shear yield strength of the matrix ( $\tau_y = \sim 16$  MPa for our microframes, a value considerably lower than the pure polymer value and one that is further tunable by tailoring the microframe geometry). The Young's modulus of the composite material can be estimated by the shear lag model<sup>[18]</sup> as

$$\frac{1}{E_c} = \frac{4(1 - V_p)}{G_m V_p^2 s^2} + \frac{1}{V_p E_p} \quad (2)$$

where  $G_m$  is the shear modulus of the matrix ( $G_m = \sim 0.3$  GPa for our microframes),  $E_p$  the Young's modulus of mineral platelets. Thus, at a given platelet concentration, the Young's modulus and tensile strength of the composite can be improved by increasing the aspect ratio of the platelets up to a critical value such that the mineral stress does not reach its strength (calculated from the ratio of yield stress of the platelet to shear strength of the matrix).<sup>[14]</sup> The effects of platelet volume fraction and platelet aspect ratio on the calculated Young's modulus and tensile strength for the structural composites are shown in **Figure 4**. Both Young's modulus and yield stress increase with the increase of  $V_p$  and  $s$ , which agrees well with the shear lag model prediction. Note that the second yield stress, which is much larger than the model prediction for higher aspect ratio cases, enables the structures to absorb much more energy. This implies that a high tensile strength can be obtained by the balanced selection of volume fraction and aspect ratio of the platelets and the polymer microframe mortar.

Returning to the case of  $V_p = 0.90$  and  $s = 10$ , these materials are also found to exhibit unique lateral strain histories during tension. **Figure 2b** shows the lateral strain and **Figure 2c** the Poisson's ratio as a function of tensile strain; the Poisson's ratio is taken to be the negative of the ratio of the increment in lateral strain to the increment in tensile strain. The lateral strain reflects contributions from the lateral strain of the mineral bricks and the microframe mortar. Prior to yield, there is essentially zero lateral straining of the mortar and therefore the Poisson ratio is primarily a result of the mineral Poisson effect, giving a small positive Poisson ratio (varying from 0.12 to 0.05, decreasing with decreasing  $V_p$ ). After first yield, a region of near zero contraction occurs (giving a near zero Poisson's ratio), which is soon followed by a dramatic lateral expansion (negative Poisson's ratio) of the composite after the second yield event. The "plastic" Poisson's ratio reaches  $-2.7$  for the structure with  $V_p = 0.90$  at a macroscopic strain of 0.006. The evolution in lateral expansion and Poisson's ratios is found to depend on the platelet volume fraction and to follow the occurrence of the yield events in the microframe (discussed later) that correspond to the macroscopic double yield events of the composite. This plastic expansion gives a volumetric straining during plastic deformation and a corresponding volumetric contribution to energy dissipation. For a material under loading, the increment of strain energy density is

$$dU = \sigma_{ij} d\epsilon_{ij} = \sigma_{ij} d\epsilon'_{ij} + \frac{1}{3} \sigma_{ij} d\epsilon \delta_{ij} \quad (3)$$

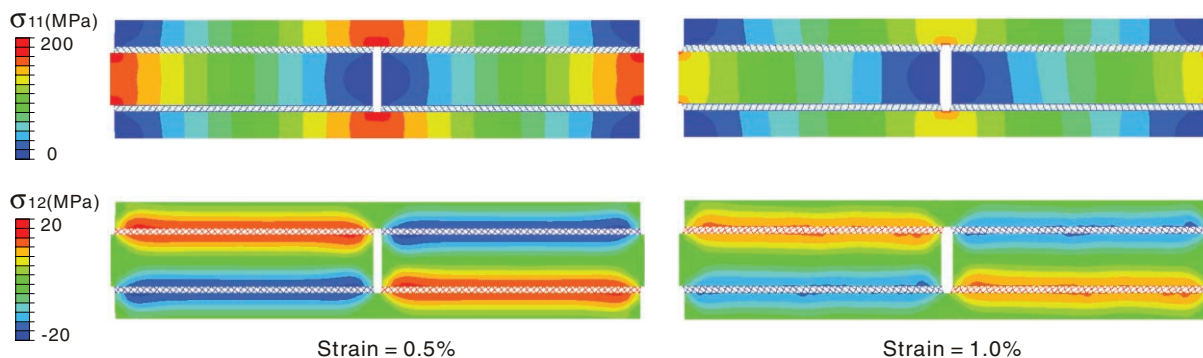


**Figure 3.** Contours of the axial stress  $\sigma_{11}$ , shear stress  $\sigma_{12}$  of the structural composite with  $V_p = 0.90$  at 0.5% and 1.0% overall tensile strain. The buildup of axial stress is a result of interfacial shear stress transmitted from the polymer microframe matrix indicating shear lag load transfer mechanism.

where  $de = d\epsilon_{11} + d\epsilon_{22} + d\epsilon_{33}$  is the increment of volumetric strain,  $d\epsilon'$  the deviatoric strain increment ( $d\epsilon'_{ij} = d\epsilon_{ij} - 1/3de\delta_{ij}$ ). The first term in Equation 3 is due to the distortion, the second term is the contribution due to the change in volume. Normally  $de = 0$  during plastic deformation since most materials are nearly incompressible during plastic deformation, indicating no volumetric energy dissipation; instead energy is dissipated through distortion deformation. In our study, the lateral plastic expansion during tension indicates that these structures can dissipate significant energy through volumetric energy dissipation before material failure, providing a new mechanism for enhancing tensile toughness and energy dissipation.

A previous study on polymer microframes<sup>[21]</sup> has found a negative normal stress develops during simple shear. A similar negative normal stress has been observed in semiflexible biopolymer networks.<sup>[24]</sup> Given that the microframe structure is locally shearing during the macroscopic tension of the composite, we postulate that this negative normal stress effect is the mechanism that governs the negative “plastic” Poisson’s ratio observed in the present structural mineral/polymer microstructure composite. To explore this underlying mechanism, simulations of the unconstrained shear behavior of the microframes are conducted. **Figure 5** depicts the mechanical response of a unit cell of the polymer microframe structure during a shear

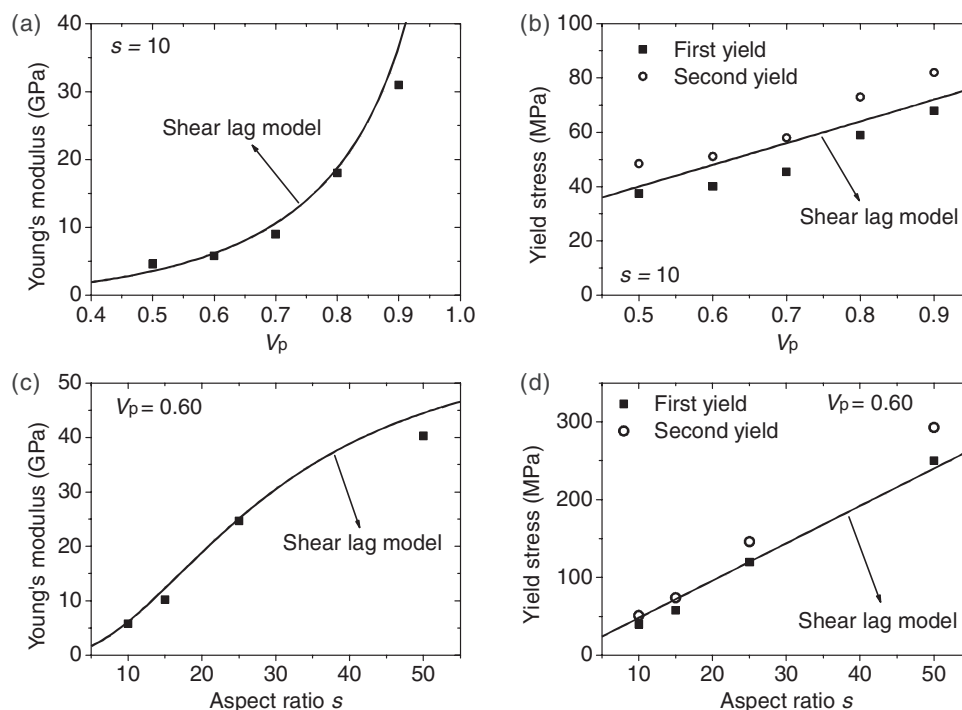


**Figure 4.** Comparison of the Young’s modulus and yield stress for the composite structure under uniaxial tension by FEA calculation (discrete point) and theoretical prediction (solid line). a) and b) Effect of platelet volume fraction on calculated Young’s modulus and yield stress for composites with  $s = 10$ , as compared to shear lag model prediction. c) and d) Effect of platelet aspect ratio on calculated Young’s modulus and yield stress for the structural composites with  $V_p = 0.60$  with comparison with shear lag theory. For reference, natural nacre with an  $s \approx 10$  and  $V_p \approx 0.95$  has a Young’s modulus of 60–90 GPa and a yield stress of  $\sim 70$  MPa.<sup>[10,17,22]</sup>

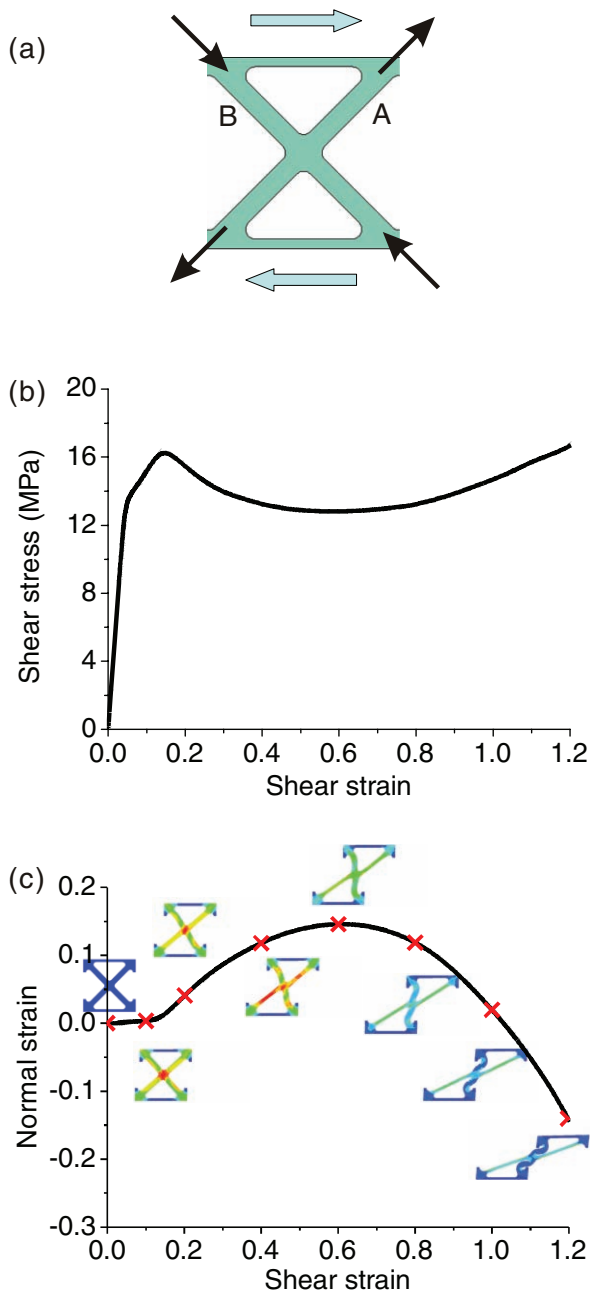


**Figure 5.** Mechanical response of polymer microframes under shear deformation. a) Schematic of a unit cell. b) Shear stress-shear strain curve. c) Normal stress-shear strain relationship and the corresponding evolution in structure with deformation.

deformation without constraint (normal traction free) in the normal direction. During shear strain of the microframe, strut A experiences simple tension, while strut B experiences compression (Figure 5a). The shear stress-shear strain and the normal strain-shear strain behavior are shown in Figure 5b and 5c, together with the deformed configurations at different levels of shear strain. At small shear strains, there is negligible normal strain as expected (this corresponds to the zero contribution to lateral expansion during elastic deformation

of the composite). The first yield event occurs in the frame junction (at a shear strain of 5%) leading to a first yield point in the shear stress-strain curve. The shear stress continues to increase until reaching the second yield point where the strut A yields because of stretching. This yielding in the junctions and then the struts leads to a double yield in the macroscopic stress-strain response of the composites. Once the yield event occurs in the struts (at a shear strain of 12%) and larger strain ensues, the normal strain is found to be positive and increasing with strain. In this region of large shear strain (from 12% to 100%), the structure expands in the normal direction. The rotation of struts during the shear enables the structure to expand to release the negative net force in the direction perpendicular to the shear direction. This expansion is caused by the force balance of the compressed and stretched struts, since there is no constraint in the normal direction. Hence, the negative “plastic” Poisson’s ratio of the composite is not a result of any auxetic-type behavior of the mortar, but is a result of its shear behavior that suggests interesting new avenues for designing microstructures to achieve mechanical performance under different loading conditions. Also, the rotation of struts reduces the net contribution to traction in the shear direction and leads to the strain softening in the shear stress-shear strain behavior as shown in Figure 5b. This explains the previous observed strain softening in Figure 2a for the composites. The compression of strut B leads to its buckling, which, in turn, leads to a peaking and subsequent decrease in the normal strain. Hence the structure begins to contract in the normal direction due to the buckling of strut B and the increasing stretch in strut A. Note that the local true strain is  $\sim 0.75$  in the polymer microframe when under a shear strain of 1.20, which is attainable for the polymer without fracture.<sup>[19,21]</sup> Therefore, the shear of polymer microframes plays a significant role in introducing a highly nonlinear response of the lateral expansion of the composite structures under tension and provides a volumetric energy dissipation mechanism during plastic deformation.

### 3. Conclusions

In summary, the large plasticity of sub-micrometer scale polymer microframes enables these cellular structures to serve as constituents in bio-inspired hierarchically structured composites and provide significant plastic dissipation capability. We have shown that these structured composites can achieve improved mechanical properties by the control of the geometry and contents of the platelets and polymer microframes. These composites are found to exhibit a negative plastic Poisson’s ratio (post-yield lateral expansion), which greatly enhances the volume energy dissipation during plastic deformation providing a significant toughening mechanism. This behavior arises as a result of highly nonlinear shear behavior of polymer microframes. Note that while other composite laminates have been shown to exhibit a negative Poisson’s ratio,<sup>[25]</sup> their behavior is a result of the layup of differently oriented lamina, is elastic, and does not provide a dissipation mechanism. However, unlike many other examples of auxetic materials<sup>[26,27]</sup> the negative plastic Poisson’s ratio is more rare and has a significant effect in promoting the plastic deformation capability and toughness of

the composite. The observed tunable negative Poisson's ratios enable these composites to have remarkable potential in the development of energy dissipative materials and a wide range of functional materials.

## Acknowledgements

This research was supported by the US Army Research Office through the Institute for Soldier Nanotechnologies under the Contract DAAD-19-02-D0002 and in part by the MRSEC Program of the National Science Foundation under award number DMR-0819762.

Received: February 10, 2010

Revised: April 5, 2010

Published online: July 29, 2010

- 
- [1] H. A. Lowenstam, S. Weiner, *On Biomineralization*, Oxford Univ. Press, New York **1989**.
- [2] U. G. K. Wegst, M. F. Ashby, *Philos. Mag.* **2004**, *84*, 2167.
- [3] A. P. Jackson, J. F. V. Vincent, R. M. Turner, *Proc. R. Soc. Lond. B* **1988**, *234*, 415.
- [4] H. Gao, B. Ji, I. L. Jager, E. Arzt, P. Fratzl, *Proc. Natl. Acad. Sci. U.S.A.* **2003**, *100*, 5597.
- [5] J. D. Currey, *Proc. R. Soc. Lond. B.* **1977**, *196*, 443.
- [6] B. L. Smith, T. E. Schaffer, M. Viani, J. B. Thompson, N. A. Frederick, J. Kindt, A. Belcher, G. D. Stucky, D. E. Morse, P. K. Hansma, *Nature* **1999**, *399*, 761.
- [7] H. J. Qi, C. Ortiz, M. C. Boyce, *J. Eng. Mater. Tech.* **2006**, *128*, 509.
- [8] H. J. Qi, B. J. F. Bruet, J. S. Palmer, C. Ortiz, M. C. Boyce, in *Mechanics of Biological Tissues, Proceedings of International Union of Theoretical and Applied Mechanics (IUTAM)*, (Eds.: G. A. Holzapfel, R. W. Ogden), Springer Verlag, Graz, Austria **2005**, 175.
- [9] M. H. Jhon, D. C. Chrzana, *J. Mech. Behav. Biomed. Mater.* **2009**, *2*, 603.
- [10] F. Song, J. B. Zhou, X. H. Xu, Y. Xu, Y. L. Bai, *Phys. Rev. Lett.* **2008**, *100*, 245502.
- [11] R. Z. Wang, Z. Suo, A. G. Evans, N. Yao, I. A. Aksay, *J. Mater. Res.* **2001**, *16*, 2485.
- [12] C. Ortiz, M. C. Boyce, *Science* **2008**, *319*, 1053.
- [13] P. Podsiadlo, A. K. Kaushik, E. M. Arruda, A. M. Waas, B. S. Shim, J. D. Xu, H. Nandivada, B. G. Pumplun, J. Lahann, A. Ramamoorthy, N. A. Kotov, *Science* **2007**, *318*, 80.
- [14] L. J. Bonderer, A. R. Studart, L. J. Gauckler, *Science* **2008**, *319*, 1069.
- [15] E. Munch, M. E. Launey, D. H. Alsem, E. Saiz, A. P. Tomsia, R. O. Ritchie, *Science* **2008**, *322*, 1516.
- [16] S. C. Zuo, Y. G. Wei, *Acta Mech. Sin.* **2008**, *24*, 83.
- [17] F. Barthelat, H. Tang, P. D. Zavattieri, C. M. Li, H. D. Espinosa, *J. Mech. Phys. Solids* **2007**, *55*, 306.
- [18] B. Ji, H. Gao, *J. Mech. Phys. Solids* **2004**, *52*, 1963.
- [19] J.-H. Jang, C. K. Ullal, T. Choi, M. C. Lemieux, V. V. Tsukruk, E. L. Thomas, *Adv. Mater.* **2006**, *18*, 2123.
- [20] M. Maldovan, C. K. Ullal, J.-H. Jang, E. L. Thomas, *Adv. Mater.* **2007**, *19*, 3809.
- [21] L. F. Wang, M. C. Boyce, C. Y. Wen, E. L. Thomas, *Adv. Func. Mater.* **2009**, *19*, 1343.
- [22] B. J. F. Bruet, H. J. Qi, M. C. Boyce, R. Panas, K. Tai, L. Frick, C. Ortiz, *J. Mater. Res.* **2005**, *20*, 2400.
- [23] B. Glavinchevski, M. Piggott, *J. Mater. Sci.* **1973**, *8*, 1373.
- [24] P. A. Janmey, M. E. McCormick, S. Rammensee, J. L. Leight, P. C. Georges, F. C. Mackintosh, *Nat. Mater.* **2007**, *6*, 48.
- [25] C. T. Herakovich, *J. Compos. Mater.* **1985**, *18*, 447.
- [26] K. E. Evans, A. Alderson, *Adv. Mater.* **2000**, *12*, 617.
- [27] R. Lakes, *Adv. Mater.* **1993**, *5*, 293.
-